

Optical coherence tomography as a diagnostic tool

Ann Singh^{1,2} and Aletta Elizabeth Karsten¹

¹ Biophotonics Group, National Laser Centre, CSIR, P.O. Box 395, Pretoria, South Africa, 0001

² Laser Research Institute, Stellenbosch University, Private bag X1, Matieland, 7602

E-mail: asingh1@csir.co.za

Abstract. Optical Coherence Tomography (OCT) has been used in biomedical applications as a method to non-invasively detect changes occurring in tissue such as the detection of skin cancer. The effect of skin tone on detection of skin cancer has however not been studied extensively. Skin simulating phantoms with different optical properties can be used to optimise a system before it can be used on patients. For this reason accurately knowing the optical properties is imperative. An Integrating Sphere system can be used to determine these optical properties. Preliminary results from phantom and human skin indicate that skin tone may influence the data obtained from OCT images.

1. Introduction

OCT is a non-invasive imaging technology based on a Michelson interferometer. It is analogous to ultrasound, however whereas ultrasound uses sound waves, OCT works on light waves, measuring the backscattering properties of tissues. The light reflected off a sample is interfered with a reference wave utilizing a technique known as low-coherence interferometry. An interference signal arises when the optical pathlength difference between the two arms of a Michelson interferometer is within the coherence length of the source. Hence, the axial resolution in OCT is proportional to the temporal coherence length of the source. OCT is an imaging technique that fills the gap between confocal microscopy and ultra-sound imaging. The typical high resolutions offered by OCT are $5\ \mu\text{m}$ although the penetration depth is currently limited to about 2-3 mm. It offers a non-destructive, non-contact, repeatable method of in vivo real time imaging at high speeds [1].

Fercher et al. [2] provide a very concise and nice description of the applications of OCT. “At present OCT is used in three different fields of optical imaging, in macroscopic imaging of structures which can be seen by the naked eye or using weak magnifications, in microscopic imaging using magnifications up to the classical limit of microscopic resolution and in endoscopic imaging, using low and medium magnification.”

OCT was first demonstrated for retinal imaging [3]. Since then it has been used in biomedical applications such as ophthalmology, gastroenterology, urology, dentistry, cardiology and dermatology among other disciplines [4-9]. Atherosclerosis plaques, which contribute to about 75% of cardiovascular diseases, have been characterised by measuring the backscattering and attenuation coefficients using OCT [4]. Distinguishing breast tumour through computational methods on OCT

images has also been done [5]. Some other studies include successfully monitoring the changes in skin after UV radiation [9] as well as in the evaluation of sun damage and pre-cancer diagnosis [10]. Other than skin cancer OCT has been applied in the field of oncology for detection of tumours in the breast, bladder, brain, gastrointestinal, respiratory, and reproductive tracts, skin, ear, nose, and throat. In many of these studies it has been able to identify the malignancy in the very early stages which often is the key to patient survival. OCT has also been explored as an imaging technique for 3-D cell activities in tissue models with the potential to extend imaging of scaffolds to in vivo applications, such as following grafting of engineered tissues into a host tissue [11].

Of particular importance to us is the use of OCT in dermatology, where OCT has been used to visualize the different layers of the skin such as stratum corneum of glabrous skin in palmoplantar locations, the epidermis and the upper dermis of skin and skin appendages and blood vessels. This has led to it being a powerful technique for skin cancer detection. Furthermore OCT has been shown to be useful in non-invasive monitoring of cutaneous inflammation etc.

The aim of our work is to determine how well our commercially bought OCT System (Swept Source OCT (SS-OCT), Thorlabs) can identify skin alterations as well as its sensitivity to the influence of skin tone on such detection.

To begin this investigation we will look at a large range of skin simulating phantoms with known optical properties i.e absorption and reduced scattering coefficients (μ_a and μ'_s). The phantoms are manufactured in-house and measured on an Integrating Sphere (IS) system [12,13]. These phantoms are then imaged using the OCT system and reconstructed to give a 3D representation of the area imaged.

2. Methodology

2.1 Preparation of phantoms

Solid resin phantoms are prepared by adding carbon black and TiO particles to a hardener-resin mixture (Aka-cure, slow, Aka-resin, Akasel) [14,15]. The phantoms are cut into discs of varying thickness. For these experiments discs with a thickness of 2mm were used.

2.2 Determination of Optical Properties

The optical properties of the phantoms are determined by using the Integrating Sphere system. In this particular case, the optical properties at 632.8 nm are determined. The calibration model at this wavelength has been validated against other models, for a He-Ne laser and a white light source(WL-S) for single sphere configurations, and shown to have low prediction errors [12,14,15]. Furthermore currently there are many therapeutic lasers with a red wavelength range. However the optical properties can be extracted for different wavelengths as we use a supercontinuum white light source (Koheras) with wavelength ranging from 500nm to 1750nm. Shown in figure 1 is the IS setup used for reflectance and transmittance measurements on the phantoms to determine the optical properties. The details of obtaining the properties are described in [12,13,16].

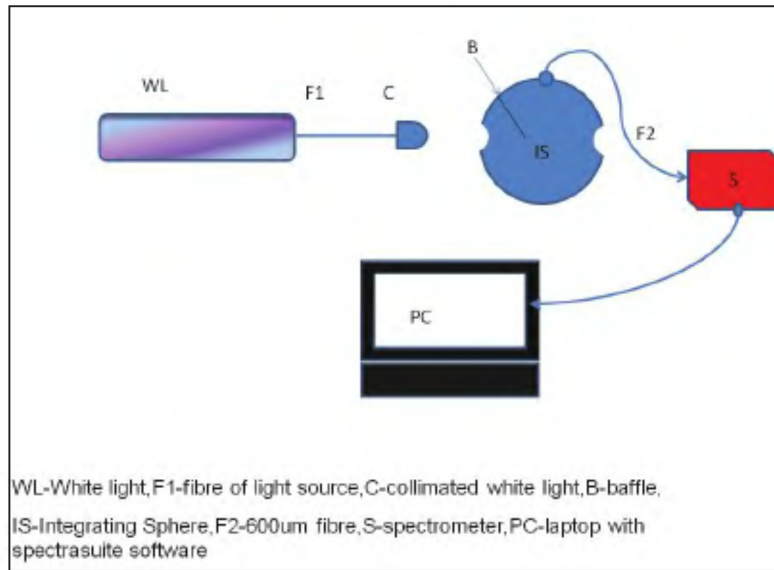


Figure 1. Single Integrating Sphere setup.

2.3 Taking an image

The system used is a Swept Source OCT (SS-OCT) with a resolution of 10-20 μm . The system is a frequency domain system with a centre wavelength of 1325nm. The magnitude and time delay of reflected light is measured and used to construct depth profiles (A-scans). Adjacent A-scans are then synthesized to create an image. The object to be scanned is placed on the path of the microscope. An volume of $10 \times 10 \times 3 \text{ mm}^3$ (x,y,z) was imaged. The contrast and brightness for all images taken was kept the same. 3D reconstructions of these images were then made.

2.4 Samples Imaged

Four 2mm phantoms with different optical properties, a 4.2mm phantom with 1mm holes, a standard pavilion and the index fingers of 2 individuals (two different skin types) were imaged.

2.5 Ethics

Ethics clearance has been obtained for this work. ETHICS REFERENCE NO: N11/01/009.

3 Results

The optical properties of the 4 phantoms were determined using the IS measurements. The measurements were done using a He-Ne laser and the white light. Table 1 shows the optical properties predicted at 632.8nm for both set of measurements. The predictions for the WL-S model are consistently higher than the He-Ne laser.

Table 1: Comparison of the predicted μ_a and μ'_s for the solid phantoms using the different models.

Sample	μ_a He-Ne	μ_a WL-S	μ'_s He-Ne	μ'_s WL-S
A1	0.041	0.05	13.27	14.50
A3	0.11	0.17	10.64	11.90
B1	0.07	0.08	5.47	6.84
B3	0.08	0.12	5.09	6.11

Based on this data these phantoms were shown to have different optical properties. These phantoms and the other objects were then imaged as described in 2.3 and 2.4. The 3D reconstructions of these images are shown in Figures (2)-(11).

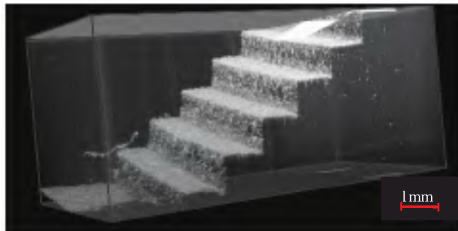


Figure 2. Pavillion.

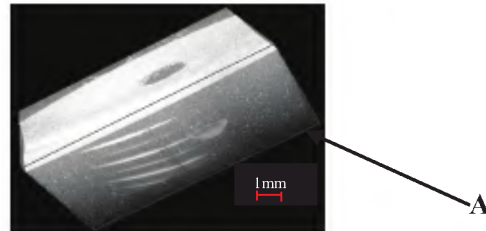


Figure 3. Phantom with holes.



Figure 4. left index top (person A).

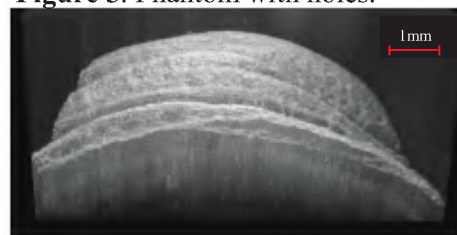


Figure 5. left index top (person B).



Figure 6. left index bottom (person A).



Figure 7. left index bottom (person B).



Figure 8. Phantom A1.



Figure 9. Phantom A3.



Figure 10. Phantom B1.



Figure 11. Phantom B3.

Figure 2 clearly shows the steps on a pavilion. Each step size is 0.5mm. This sample is used as a quick test to confirm that the system is working properly. Figure 3 shows the 4.2mm phantom with a hole. Although one can clearly see the hole with the eye, the depth of the hole is not visible to the eye. However reconstructing the image shows us the depth of the hole (point A). Currently the depth has not been evaluated, however this image shows us that it may be possible to view and determine the depth of an object such as a tumour imbedded in skin. Figures 4 and 5 compare the images, taken from the topside, on the left index finger of A and B. Figures 6 and 7 compare the images, taken from the bottom, on the left index finger of A and B. Figures 7 and 5 show more clearly defined layers of the skin than seen in figures 4 and 6. This suggests to us that the skin tone may influence the images

obtained by OCT. However such conclusions can only be made once a study of a larger data set is done. Furthermore one would need to determine whether the differences are due to skin tone or age, skin structure etc. The differences in the images obtained for the same person show that the area imaged also influences the data due to the composition of the skin in the area.

Phantom B1 (Figure 10) appears to show the most detail through the sample and phantom A3 (Figure 9) the least. Phantom B1 has the third lowest absorption and scattering properties whereas phantom A3 has the highest absorption and second highest scattering properties. Phantom B3 with the lowest scattering and second highest absorption properties shows more clarity than phantoms A1 and A3. Finally phantom A1 (Figure 8) with the lowest absorption and highest scattering appears to show a little more detail than phantom A3. These results are interesting because OCT is based on the scattering properties of samples. It is the light reflected of the sample that creates the image seen. However these results show that both the absorption and scattering properties influence the images. These are encouraging results but need to be re-evaluated with a much larger study.

4 Conclusions

These preliminary findings support our hypothesis that skin tone may influence the OCT images obtained. It is premature to state that we have proven our hypothesis to be true until the larger study has been completed.

Acknowledgments

We would like to acknowledge Bafana Moya for preparing the phantoms used in these experiments.

References

- [1] Levitz D, Thrane L, Frosz M, Andersen P, Andersen C, Andersson-Engels S, Valanciunaite J, Swartling J, and Hansen P 2004 *Opt. Express* **12** 249
- [2] Fercher, AF, Drexler W, Hitzinger CK and Lasser T 2003 *Rep. Prog. Phys.* **66** 239
- [3] Huang D, Swanson E A, Lin CP, Schuman JS, Stinson WG, Chang W, Hee MR, Flotte T, Gregory K, Puliafito CA and Fujimoto JG 1991 *Science* **254** 1178
- [4] Faber D, van der Meer F, Aalders M and van Leeuwen T 2004 *Opt. Express* **12** 4353
- [5] Zysk AM, Nguyen FT, Oldenburg AL, Marks DL and Boppart SA Oct 2007 *J. Biomed. Opt.* **12** 051403
- [6] Chenyang Xu, Joseph M. Schmitt, Stephane G. Carlier and Renu Virmani 2008 *J. Biomed. Opt.* **13**(3) 034003
- [7] Mujat M, Ferguson RD, Hammer DX, Gittins C and Iftimia N 2009 *J. Biomed. Opt.* **14** 034040
- [8] Mogensen M, Nürnberg B, Forman J, Thomsen J, Thrane L and Jemec G 2009 *British Journal of Dermatology* **160** 1026
- [9] Gambichler T, Boms S, Stucker M, Moussa G, Kreuter A, Sand M, Sand D, Altmeyer P and Hoffmann K 2005 *Arch Dermatol Res* **297** 218
- [10] Korde VR, et al. 2007 *Lasers Surg Med* **39** 687
- [11] Tan W, Oldenburg AL, Norman JJ, Desai TA and Boppart SA 2006 *Optics Express* **14** 7159
- [12] Singh A, Karsten AE 2011 *Proc. SPIE* 8192, 81924Z-1
- [13] Singh A, Karsten AE and Dam JS 2008 *Proc. of the World Association of Laser Therapy (WALT)*, Sun City, South Africa 4
- [14] Karsten AE, Singh A and Braun MW (published online April 2011) *Lasers Med Sci*, DOI 10.1007/s10103-011-0926-x
- [15] Karsten AE and Singh A 2011 *Proc. of SPIE* Vol. **8192** 81924U-1
- [16] Singh A, Karsten AE, Mputle I, Chetty A and Naidoo K 2009 *Proc. SPIE* **7373** 737317 doi:10.1117/12.831882